Journal of Power Sources 214 (2012) 153–158

Contents lists available at SciVerse ScienceDirect

Journal of Power Sources

journal homepage: www.elsevier.com/locate/jpowsour

Electrophoretic deposition of bi-layered LSM/LSM-YSZ cathodes for solid oxide fuel cell

Yoshiteru Itagaki [a,*], Shinji Watanabe [a], Tsuyoshi Yamaji [b], Makiko Asamoto [a], Hidenori Yahiro [a], Yoshihiko Sadaoka [a]

[a] Department of Materials Science and Engineering, Graduate School of Science and Engineering, Ehime University, 3 Bunkyo-cho, Matsuyama 790-8577, Japan
[b] Department of Chemical Engineering, Shikoku Research Institute Inc., 2109-8 Yashima Nishi-machi, Takamatsu 761-0192, Japan

HIGHLIGHTS

- Bi-layered SOFC cathode was first prepared by EPD technique.
- Dependence of thicknesses of the layers on cathodic resistances was investigated.
- The optimal thickness of the LSM-YSZ layer was 4 μm at 600 °C.
- Cathode property at 800 °C mainly depended on the thickness of LSM layer.

ARTICLE INFO

Article history:
Received 24 January 2012
Received in revised form
4 March 2012
Accepted 26 April 2012
Available online 4 May 2012

Keywords:
Electrophoretic deposition
SOFC
Cathode
Bi-layer
Thickness

ABSTRACT

Bi-layered cathodes with the LSM/LSM-YSZ structure for solid oxide fuel cells were successfully formed on the carbon-sputtered surface of a YSZ sheet by electrophoretic deposition (EPD). The thicknesses of the first layer of LSM-YSZ (LY) and the second layer of $La_{0.8}Sr_{0.2}MnO_3$ (LSM) could be controlled by adjusting the deposition time in the EPD process. The cathodic properties of the bi-layered structures were superior to those of the mono-layered structures, and were dependent on the thickness of each layer. Decreasing the thickness of the first layer and increasing that of the second layer tended to reduce both polarization and ohmic resistances. The optimal thickness of the first layer at the operating temperature of 600 °C was 4 μm, suggesting that an effective three-phase boundary was extended from the interface between the electrolyte and cathode film to around 4 μm thickness.

1. Introduction

Solid oxide fuel cells (SOFCs) are expected to be the next generation of distributed power generators because of their high-energy conversion efficiency without using noble metals, and also their operation capability using low purity hydrogen containing CO. The main limitations of SOFCs, restricting their broad commercialization, are their relatively low durability and the narrow selectivity of materials associated with the high operation temperature. Therefore, the major goal of SOFC development is to reduce the operation temperature to below 800 °C. It is now feasible to reduce ohmic resistance of a solid electrolyte by adopting highly conductive materials and their thin films [1–3]. Reducing electrode resistance, especially cathodic resistance, is a key factor in reducing the operation temperature. It is widely accepted that a composite cathode, where an electrolyte component is added as a secondary phase into a conventional cathode material, such as $La_{0.8}Sr_{0.2}MnO_3$ (LSM), can effectively reduce cathodic polarization resistance [4–8]. LSM-YSZ is the conventionally used material for a composite electrode [4–6]. Adding YSZ into LSM is believed to increase the number of interfaces between LSM and YSZ, and extend the three-phase boundary (TPB) from the interface between the electrolyte and electrode to interior of the electrode layer. On the other hand, adding YSZ could cause an increase in ohmic resistance of the cathode because the electron conductivity of YSZ is much lower than that of LSM [9]. An increase in electrode thickness will increase the total number of interfaces along the thickness direction of the electrode layer. However, the number of effective reaction sites of oxygen is not necessarily proportional to the electrode thickness; it will depend on the microstructure of the electrode [10]. If the thickness of the composite electrode is larger than the thickness of

* Corresponding author. Tel./fax: +81 89 927 9755.
E-mail address: itagaki@eng.ehime-u.ac.jp (Y. Itagaki).

0378-7753/$ – see front matter © 2012 Elsevier B.V. All rights reserved.
doi:10.1016/j.jpowsour.2012.04.079

the effective reaction layer, the remaining part of the composite electrode will not function sufficiently; rather it just acts as an electron-conducting layer with high resistance. In such a case, it is reasonable that a current collective LSM layer substitutes for the poorly functioning part in the composite electrode. Antunes et al. [14] previously prepared LSM/LSM-YSZ bi-layered cathodes with different thicknesses of each layer by screen-printing. They concluded that the optimal thickness of the LSM-YSZ layer was 6–12 μm. So far, several methods have been applied for preparing multi-layered cathode films, such as screen-printing [14–17], spray coating [18,19], and chemical vapor deposition [20]. In order to understand the properties of a bi-layered cathode in this study, we created the LSM/LSM-YSZ bi-layered structure by adopting the electrophoretic deposition method (EPD). This technique has also been applied for SOFC fabrication, mainly for thin electrolyte film preparation [11–13]. EPD is a very simple technique and is effective for controlling film thickness. We thus prepared bi-layered structures of the cathode with different combinations of thickness of each layer.

2. Experimental

2.1. Preparation of LSM and LSM-YSZ powders

$La_{0.8}Sr_{0.2}MnO_3$ (LSM) was prepared by the Pechini process [21]. First, stoichiometric molar amounts of $La(NO_3)_3{\cdot}6H_2O$, $Sr(NO_3)_2$ and $Mn(NO_3)_2$ were dissolved in water containing ethylene glycol and citric acid. Heating the solution to 90 °C yielded a gelated precursor. Then, the precursor was calcinated at 1000 °C for 1 h to obtain LSM crystalline powder. The obtained LSM powder was further ball-milled in methanol for 24 h to yield a fine powder. The surface area of the final product was 6.14 $m^2\ g^{-1}$ evaluated with a BET analysis. The YSZ powder was purchased from Tosoh Co. Ltd. (TZ-8Y). In our examination with a BET analysis, the surface area of the YSZ powder was evaluated to be 15.7 $m^2\ g^{-1}$. The LSM-YSZ composite powder was prepared as follows. LSM powder was prepared by calcination of the precursor at 600 °C, and mixed with equivalent weight of YSZ powder and a small amount of 3% PVA aqueous solution. This mixture was uniaxially pressed into pellets under 10 MPa pressure and calcined at 1000 °C for 1 h. The calcined pellets were pulverized into fine powder by ball-milling in methanol. The specific surface areas of both powders were evaluated using BET analysis to be 15.5 and 15.0 $m^2\ g^{-1}$, respectively.

2.2. Cathode formation by EPD

Cathode films were formed on the carbon-deposited surface (0.5 × 0.5 cm^2) of an 8 mol% YSZ sheet. The thickness of the YSZ sheet was 0.2 mm. 0.1 g of LSM or LSM-YSZ powder was added into 10 mL of acetylacetone containing 0.015 g of I_2 as a charging agent. The mixtures were subjected to ultrasonic agitation for 20 min to obtain a stable suspension. The carbon-deposited YSZ sheet and stainless sheet were soaked in the suspension. The distance between the electrodes was fixed at 1.0 cm. EPD was carried out by applying a constant dc voltage of 15 V. The binary-layers were prepared as follows. First, LSM-YSZ was deposited using the LSM-YSZ suspension for a set time. After drying, LSM was deposited on the LSM-YSZ deposited surface in the LSM suspension. The cathode films were sintered at 1000 °C for 1 h. The thickness of each layer was determined by SEM-EDX observation.

2.3. Cell preparation and cathodic examinations

After cathode formation, Pt-paste was screen printed on the same side (reference electrode) and the other side (anode) of the YSZ sheet and sintered at 600 °C for 1 h. The areas of the cathode, anode and reference electrodes were 0.25, 0.25, and 0.1 cm^2, respectively. The top of cathode was totally covered with a porous Pt thin film as a terminal current collector, and the Pt film was wired with Pt–lead. The three-terminal cell configuration and the setup used for the cell test are shown in Fig. 1. For cell tests, the cathode and counter sides were exposed to compressed air and humidified 3% H_2/Ar, respectively. The voltage between the cathode and the reference, ΔV_{C-R}, was measured for different values of constant current between the cathode and anode in the temperature range between 600 and 800 °C. The current was controlled with an electronic load (Takasago; FK-160L2Z). Furthermore, the resistance components, *i.e.*, ohmic and overpotential resistances, contained in ΔV_{C-R} were separately evaluated with current interruption during the SOFC operation. In order to evaluate YSZ-adding effect on ohmic resistance of LSM, dc resistance was measured for the LSM and LSM-YSZ sinters. The compacted disks sintered at 1100 °C were cut into cubes and attached with Pt electrodes to be a configuration for four-probe dc measurement.

3. Results and discussion

3.1. Mono-layered cathodes

Mono-layered cathode films of LSM and LSM-YSZ were first examined. The film thickness after the sintering process was proportional to the deposition time at a constant voltage of 15 V cm^{-1}. Fig. 2 shows the cathodic potential drop of the series of the mono-layered cathodes with different thicknesses observed at 600 and 800 °C. In the figure the mono-layered cathodes of LSM and LSM-YSZ are denoted as LSM and LY, respectively, along with the values of thickness in μm (e.g., a LSM cathode with 8 μm thickness is denoted as "LSM8"). In both cathodes, the cathodic potential drop tends to be suppressed with increasing film thickness. The cathodic resistance components of these cathodes evaluated by the current interruption method are shown in Table 1. In both LSM and LSM-YSZ cathodes, increasing thickness tends to reduce ohmic and polarization resistances. The ohmic drop assigned to an electrode can be divided into in-plane and cross-plane drops. Here cylindrical pores are assumed to be present at the interface between electrode and porous current collector. The pores does not directly contact with the current collecting layer. When integration of the above pores over the electrode surface can be considered as a single pore with radius *r*, in-plane ohmic drop can be described and cross-plane ohmic drop can be expressed as following equation [22,23]:

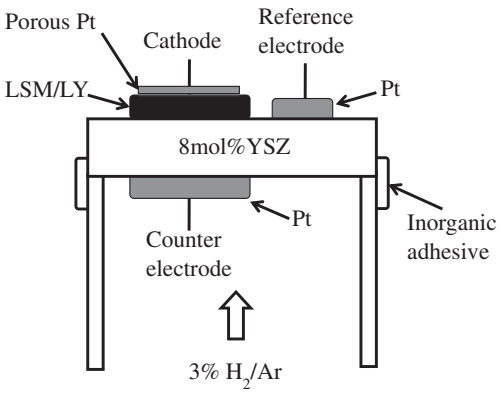

Fig. 1. The cell configuration used in the measurements for cathodic properties.

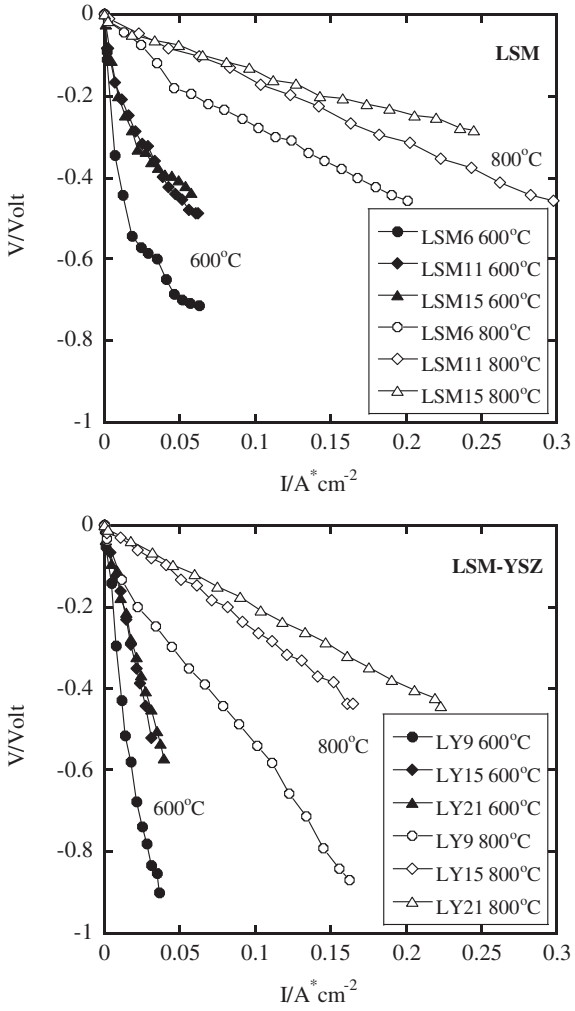

Fig. 2. Cathodic potential drop vs. applied current density measured for the LSM and LSM-YSZ cathodes with different thicknesses at 600 and 800 °C.

$$U_{\text{in-plane}} = (\rho_e i/4\text{th}) \times r^2 \quad (1)$$

$$U_{\text{cross-plane}} = \rho_e \times i \times \text{th} \quad (2)$$

where U = ohmic drop, i = current density, ρ_e = resistivity of electrode, th = thickness of electrode, and r = radius of the cylindrical pores. The ohmic drops are inversely proportional and directly proportional to thickness of electrode, respectively. Therefore, the decreases in ohmic drop with increasing electrode thickness, which can be commonly seen in the LSM and LSM-YSZ cathodes, are probably due to that a decrease in in-plane ohmic resistance is beyond an increase in cross-plane ohmic resistance.

Meanwhile, polarization drop may be related to the number of reaction sites. In the case of the LSM cathode, the reaction sites are limited at near interface between electrode and electrolyte because ionic conductance of LSM is negligibly small. In this case, the LSM layer is exclusively used for an electron migration pathway. Therefore, electronic migration resistance in LSM cathode seems to be an important factor for the polarization drop. The decrease in the polarization drop with increasing electrode thickness is probably due to the enhancement of the in-plane electronic conduction. On the other hand, the number of reaction sites in the LSM-YSZ cathode is expected to increase to some extent with increasing thickness. The effective thickness for cathodic reaction would depend on electronic and ionic migration resistances in LSM-YSZ.

The decrease in cathodic potential of the LSM-YSZ cathodes appeared to be larger compared to those of the LSM cathodes. This difference was more significant at 800 °C. Since the electronic conductivity of YSZ is almost negligible at $p(O_2) = 1$ compared to that of LSM (200 S cm^{-1} at 800 °C [24]), the high ohmic resistance of the LSM-YSZ cathode was probably due to the fact that the electronic conduction path through the electrode thickness was partially obstructed by the addition of YSZ [9]. It should be noted that the polarization resistance of LSM-YSZ was lower than that of LSM. Therefore, the addition of the YSZ phase has a certain degree of contribution to enhance the ionic conductivity of LSM-YSZ. In order to verify the increase in ohmic resistance by the added YSZ, conductivities of LSM and LSM-YSZ were evaluated by the dc four-probe method. Fig. 3 shows the temperature dependence of the dc conductivities of the materials sintered at 1100 °C. Conductivity decreased remarkably with increasing YSZ content. The activation energies evaluated from the line slopes were 8.29 (LSM), 8.90 (LSM-YSZ 70:30), and 10.55 kJ mol^{-1} (LSM-YSZ 50:50). Since the whole conductivity of those bulks is governed by electronic conductivity of LSM, the addition of YSZ probably increased the activation energy of a percolation conductance.

Table 1
The cathodic resistance components of the series of the mono-layered cathodes with different thicknesses at 600 and 800 °C.[a]

	Resistances/Ω cm^2					
	600 °C			800 °C		
	R_Ω	R_p	Total	R_Ω	R_p	Total
LSM6	3.96	25.5	29.5	2.10	1.58	3.68
LSM11	2.66	19.6	22.3	1.50	0.58	2.08
LSM15	1.47	13.3	14.8	1.21	0.42	1.63
LY9	18.3	12.3	30.6	4.33	0.86	5.19
LY15	15.0	1.90	16.9	2.44	0.33	2.77
LY21	13.2	1.13	14.3	1.92	0.18	2.10

[a] The polarization resistances (R_p) were evaluated from an initial slope of the i–v curves on cathodic polarization drops.

3.2. Bi-layered cathodes

Bi-layered cathode structures, where LSM-YSZ and LSM were deposited as the first and second layers (denoted as LSM/LY with

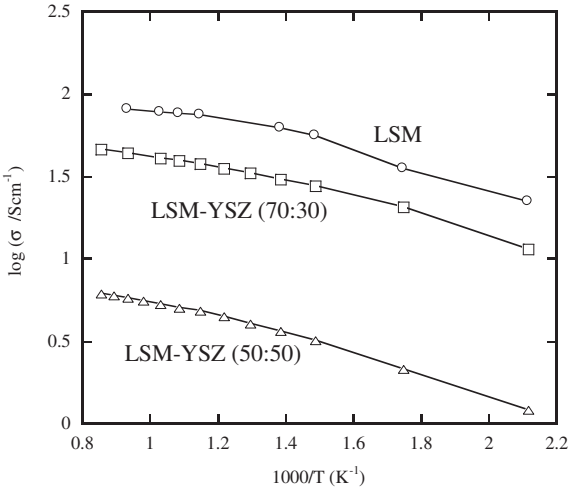

Fig. 3. Temperature dependence of the dc conductivity measured for LSM and LSM-YSZ bulks sintered at 1100 °C. The two types of LSM-YSZ are those containing weight ratios of LSM and YSZ at 70:30 and 50:50, respectively.

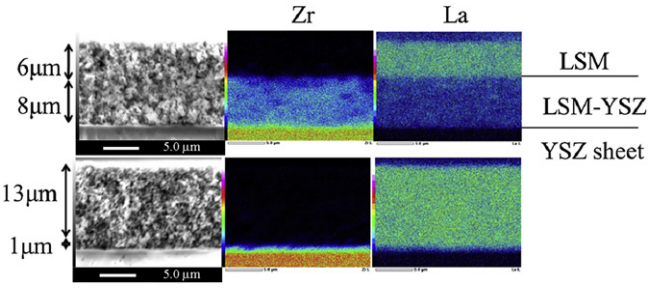

Fig. 4. Zr- and La-elemental mappings of the fractured surfaces of the bi-layered cathodes, LSM6/LY8 and LSM13/LY1, observed by SEM-EDX.

each respective thickness in μm), were formed by two-step deposition. The elemental distribution of zirconium and lanthanum through the fractured surface of the cathode films showed that bi-layered structures were successfully formed (Fig. 4). The fractured surfaces of the bi-layered structures were also observed by high resolution SEM. The SEM micrograph of LSM6/LY8 is shown in Fig. 5. The bi-layered structure appeared to consist of relatively dense LY and porous LSM layers. At first, the LY layer with a thickness of 8 μm and LSM layers with different thicknesses were deposited as first and second layers, respectively. The cathodic properties of these bi-layered cathodes are shown in Fig. 6. LSM6/LY8 exhibited better cathodic properties than the mono-layered LSM cathode at 600 °C. It was deduced that inserting the LY8 layer into the LSM layer would increase the number of reaction sites and the LSM6 second layer would function as an oxygen-supplying and current collecting layer. Increasing the thickness of the LSM layer to 12 and 18 μm further enhanced the cathodic properties. The cathodic resistance components of these cathodes evaluated by the current interruption method are shown in Table 2. Increasing the LSM thickness reduced both ohmic and polarization resistances. In particular, the change in ohmic resistance was remarkable, varying from 6 to 12 μm at 600 °C. This result may correspond to the reduction of the ohmic resistance of the mono-layered LSM cathode by varying the thickness from 6 to 11 μm, and increasing the thickness may enhance the current collecting effect. At 800 °C, the variation in the resistance became rather small compared to that at 600 °C.

Next, reduction in the thickness of the first layer, LY, was considered. The thickness of the LY layer was reduced to 4, 2 and 1 μm. SEM-EDX analysis for LSM13/LY1 is shown in Fig. 4. A flat interface between the two layers was achieved even for such small thicknesses with the current conditions of EPD. The cathodic properties of the series of bi-layered cathodes are shown in Fig. 6. Despite the thickness of the LSM layer being smaller than that of LSM18/LY8, all the cathodes with thinner LY layers exhibited better

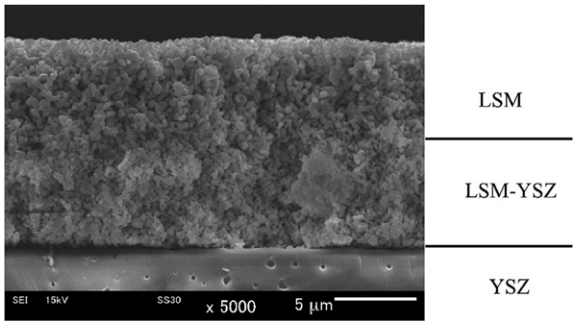

Fig. 5. SEM micrograph of the fractured surface of bi-layered LSM6/LY8 cathodes.

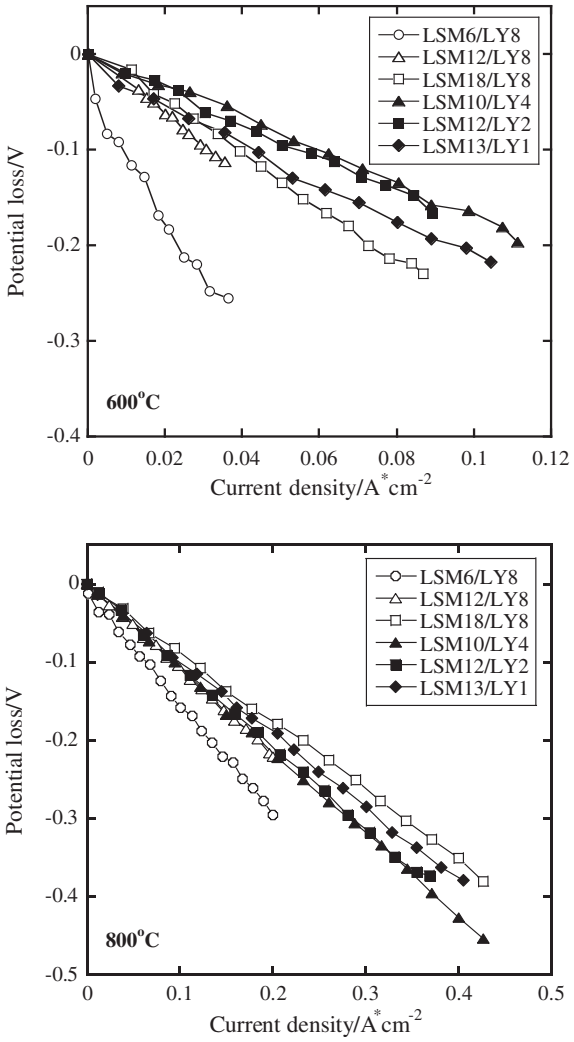

Fig. 6. Cathodic potential drop vs. applied current density measured for the series of bi-layered cathodes at 600 and 800 °C.

properties than those of LSM18/LY8 at 600 °C. Reducing the thickness of the first layer was even more effective in enhancing the cathodic properties than increasing the thickness of the second layer at 600 °C. The resistance components of these cathodes are summarized in Table 2. Thinning the thickness of the first layer below 8 μm seems to reduce both ohmic and polarization resistances. This fact appears to be contradictory to the result of the mono-layered LSM-YSZ (Fig. 2), where thickening the thickness

Table 2
The cathodic resistance components of the series of the bi-layered cathodes at 600 and 800 °C.[a]

	Resistances/Ω cm^2					
	600 °C			800 °C		
	R_Ω	R_p	Total	R_Ω	R_p	Total
LSM6/LY8	5.18	2.00	7.18	1.43	0.13	1.56
LSM12/LY8	2.05	1.95	4.00	1.03	0.10	1.13
LSM18/LY8	1.30	1.53	2.83	0.83	0.03	0.86
LSM10/LY4	1.20	0.55	1.75	1.05	0.08	1.13
LSM12/LY2	0.98	0.98	1.96	0.98	0.08	1.06
LSM13/LY1	1.00	1.00	2.00	0.93	0.05	0.98

[a] The polarization resistances (R_p) were evaluated from an initial slope of the i–v curves on cathodic polarization drops.

reduces the ohmic resistance. Probably, in the case of the first layer of the bi-layered cathode, the cross-plane resistance, which reduces with decreasing film thickness, is dominantly contributing in the first layer. Variation of the both resistance drops to the film thickness can be described as differentials of the ohmic drops with respect to thickness;

$$dU_{\text{in-plane}}/dth = \left(-\rho_e i/4th^2\right) \times r^2 \quad (3)$$

$$dU_{\text{cross-plane}}/dth = \rho_e \times i \quad (4)$$

and the sum of the above differentials is the variation of the total resistance drop, U_{total}, depending on the thickness;

$$dU_{\text{total}}/dth = \rho_e i\left\{1 - (r/2th)^2\right\} \quad (5)$$

When dU_{total}/dth is negative, *i.e.*, $r > 2th$, in-plane resistance would be more largely dependent on the thickness, and by contraries when dU_{total}/dth is positive, *i.e.*, $r < 2th$, cross-plane resistance would be more largely dependent on the thickness. In the case of the mono-layer, r is practically radius of a pore at the interface between the LSM-YSZ cathode and the porous Pt layer, but in the case of the bi-layer, r is associated to radius of a pore at the interface between the LSM-YSZ cathode (first layer) and the current collecting LSM layer (second layer). It can be speculated that r of the pores at the interface between the LSM-YSZ cathode and porous Pt layer in the mono-layered structure is larger than that between the first and second layer in the bi-layered structure, and in the case of the bi-layered structure equation (5) would be positive. Therefore, the cross-plane resistance is deduced to be the main component in the LSM-YSZ layer in the bi-layered cathode, and the overall resistance decreases with decreasing the thickness.

For the polarization drop, thinning the first layer below 8 μm was more effective than thickening the second layer. The overpotential drop became minimum at 4 μm and again increased by further thinning. Barbucci et al. [10] previously investigated the influence of the thickness of an LSM-YSZ composite electrode in the range between 5 and 100 μm, and they observed a decrease in the cathodic resistance with increasing thickness up to about 40 μm. They assumed two types of current paths to approximately interpret their results; they also assumed that oxygen gas was present in the electrode pores and neglected oxygen adsorption and diffusion. Of the two current paths suggested by Barbucci et al., one is a "surface path" where the cathodic reaction takes place at the true interface between the dense electrolyte and electrode, and electrons migrate through the electrode thickness. In this path, polarization resistance will be divided into electron migration and charge transfer resistances, and only the electron migration resistance depends on the thickness. Since the cross-plane resistance, which decreases by thinning the thickness, is dominant on the first layer (LSM-YSZ), the resistance for the surface path (R_s) would monotonously decrease by thinning the thickness. Therefore this path cannot solely explain the optimal thickness of the first layer (4 μm) obtained in this study. The other current path is a "volume path" where the reaction takes place at an intermediate thickness, and electrons and ions migrate in opposite directions each other through the thickness. In this path, electron and ionic migration resistances will increase and charge transfer resistance will decrease with decreasing the thickness. Therefore the resistance for the volume path (R_v) will be balanced with those resistance components. The total polarization resistance (R_p) can be described as:

$$R_p = \frac{R_s R_v}{R_s + R_v} \quad (6)$$

Now we assume that current mainly pass through the volume path and the charge transfer reaction would take place at 4 μm above the true interface between the electrode and the electrolyte layers. When the total thickness of the LSM-YSZ layer is larger than 4 μm, electron should migrate through the residual upper part of the LSM-YSZ layer. Therefore, the residual part of the LSM-YSZ layer should be replaced with LSM layer with a lower ohmic resistance. When the thickness is smaller than 4 μm, the charge transfer reaction will take place at the interface between the LSM-YSZ and LSM layers. In this case, electron can only migrate through the LSM layer. However, this reduction in the thickness would make the reduction in the number of reaction sites dominant over the reduction in the electron migration resistance. Consequently, it follows that LSM10/LY4 is an optimized structure. At 800 °C, the order of the cathodic properties changed to LSM13/LY1 > LSM12/LY2 > LSM10/LY4. Furthermore, LSM18/LY8 exhibited the best properties at this temperature. Therefore, the thickness of the second layer is likely to be a decisive parameter for cathodic properties. However, the situation is different at 800 °C, where polarization resistance is a minor component and the cathodic properties are almost governed by ohmic resistance. In this sense, LSM13/LY1 has the potential to have enhanced properties by further increasing LSM thickness. It should be noted that the LY-layered free electrode, also known as the mono-layered LSM, has lower properties than LSM13/LY1. Therefore, even the existence of a 1 μm thick LY layer contributes significantly to the increased number of oxygen reaction sites. Thus, the bi-layered cathode exhibited better performance compared to the mono-layered cathode, and LSM10/LY4 and LSM18/LY8 were the optimal structures at 600 and 800 °C, respectively. It was suggested, by the above-mentioned results, that the effective thickness of the oxygen reaction in the LY layer would be a decisive factor for cathode performance. The effective thickness determines the thickness for electron and ion migrations and the number of reaction sites. The effective thickness would vary with the thickness of the LSM layer and the morphology of the LY layer, porosity and grain-boundary structure.

4. Conclusion

SOFC cathodes with bi-layered structures of LSM/LSM-YSZ were prepared using EPD. The thickness of each layer could be well-controlled by adjusting the deposition time in the EPD process. The bi-layered structures exhibited lowered cathodic potential loss compared to the mono-layered structures. The decrease in thickness of the first layer and the increase in thickness of the second layer effectively reduced both polarization and ohmic resistances. Among the examined bi-layered structures, LSM10/LY4 exhibited the minimal polarization resistance at 600 °C. It was deduced that the effective thickness of the active layer is around 4 μm under the current conditions.

Acknowledgments

This study was subsidized and supported by the Mazda Foundation.

References

[1] U.B. Pal, S.C. Singhal, J. Electrochem. Soc. 137 (1990) 2937–2941.
[2] Z. Ogumi, Y. Uchimoto, Y. Tsuji, Z. Takehara, J. Appl. Phys. 72 (1992) 1577–1582.
[3] A.R. Nicoll, A. Salito, K. Honegger, Solid State Ionics 52 (1992) 269–275.
[4] T. Kenjo, M. Nishiya, Solid State Ionics 57 (1992) 295–302.
[5] E.P. Murray, T. Tsai, S.A. Barnett, Solid State Ionics 110 (1998) 235–243.

[6] M.J. Jørgensen, S. Primdahl, M. Mogensen, Electrochem. Acta 44 (1999) 4195–4201.
[7] G. Dotelli, C.M. Mari, R. Ruffo, P. Pelosato, I.N. Sora, Solid State Ionics 177 (2006) 1991–1996.
[8] Z. Wang, M. Cheng, Y. Dong, Min Zhang, H. Zhang, Solid State Ionics 176 (2005) 2555–2561.
[9] D. Kim, G.D. Kim, J.W. Moon, Y. Park, W.H. Lee, K. Kobayashi, M. Nagai, C.E. Kim, Solid State Ionics 143 (2001) 379–389.
[10] A. Barbucci, M. Carpanese, A.P. Reverberi, G. Cerisola, M. Blanes, P.L. Cabot, M. Viviani, A. Bertei, C. Nicolella, J. Appl. Electrochem. 38 (2008) 939–945.
[11] T. Ishihara, K. Sato, Y. Takita, J. Am. Ceram. Soc. 79 (1996) 913–919.
[12] I. Zhitomisky, A. Petric, J. Eur. Ceram. Soc. 20 (2000) 2055–2061.
[13] K. Yamaji, H. Kishimoto, Y. Xiong, T. Horita, N. Sakai, H. Yokokawa, Solid State Ionics 175 (2004) 165–169.
[14] R. Antunes, T. Golec, M. Miller, R. Kluczowski, M. Krauz, K. Krzastek, J. Fuel Cell Sci. Technol. 7 (2010) 0110111–0110116.
[15] N.T. Hart, N.P. Brandon, M.J. Day, J.E. Shemilt, J. Mater. Sci. 36 (2001) 1077–1085.
[16] X. Xu, C. Xia, G. Xiao, D. Peng, Solid State Ionics 176 (2005) 1513–1520.
[17] H.S. Song, S. Lee, D. Lee, H. Kim, S.H. Hyun, J. Kim, J. Moon, J. Power Sources 195 (2010) 2628–2632.
[18] N.T. Hart, N.P. Brandon, M.J. Day, N. Lapeña-Rey, J. Power Sources 106 (2002) 42–50.
[19] P. Holtappels, C. Bagger, J. Eur. Ceram. Soc. 22 (2002) 41–48.
[20] Y. Liu, C. Compson, M. Liu, J. Power Sources 138 (2004) 194–198.
[21] M. Liu, D. Wang, J. Mater. Res. 10 (1995) 3210–3221.
[22] M. Kleitz, F. Petitbon, Solid State Ionics 92 (1996) 65–74.
[23] J.D. Kim, G.D. Kim, J.W. Moon, H.W. Lee, K.T. Lee, C.E. Kim, Solid State Ionics 133 (2000) 66–67.
[24] J. Mizusaki, Y. Yonemura, H. Kamata, K. Ohyama, N. Mori, H. Takai, H. Tagawa, M. Dokiya, K. Naraya, T. Saamoto, H. Inaba, T. Hashimoto, Solid State Ionics 132 (2000) 167–180.